

Supplemental information

**Establishment of a microwell-array-based
miniaturized thymic organoid model
suitable for high-throughput applications**

Viktoria Major, Sam Palmer, Paul Rouse, Jan Morys, Timothy Henderson, Tania Hübscher, Joanna Sweetman, Andrea Bacon, Chengrui An, Qiu Guiyun, Yu Wang, Andrea Corsinotti, Justyna Cholewa-Waclaw, S. Jon Chapman, Matthias P. Lütolf, Graham Anderson, and C. Clare Blackburn

Supplemental Figures

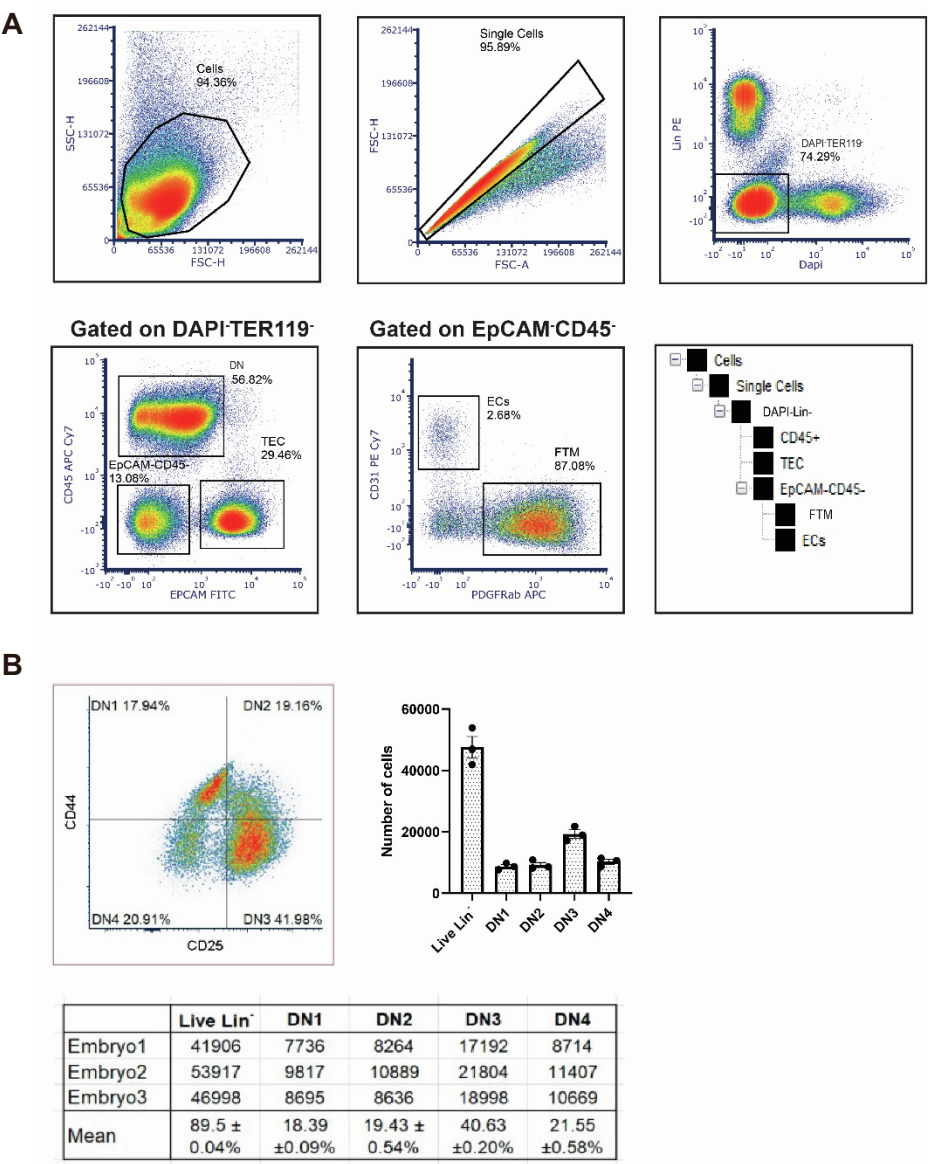


Figure S1. Cellular composition of the E14.5 thymus. A) Plots show gating strategy for isolating TEC, DN thymocytes, FTM and ECs from E14.5 thymic lobes. TEC were sorted from single cells as DAPI-TER119⁻CD45⁻EpCAM⁺ cells, DNs as DAPI-Lin⁻CD45⁺EpCAM⁻ cell, FTM as DAPI-TER119⁻CD45⁻EpCAM⁺PDGFRα⁺ cells and ECs as DAPI-TER119⁻CD45⁻EpCAM⁺PDGFRα⁺CD31⁺ cells. B) Representative plot showing the CD44 versus CD25 subset profile, absolute cell numbers and percentages for E14.5 DAPI-Lin⁻CD45⁺ cells. Lin = α-CD4, α-CD8, α-CD11b, α-CD11c, Gr1, NK1.1, B220, TER-119, α-EpCAM.

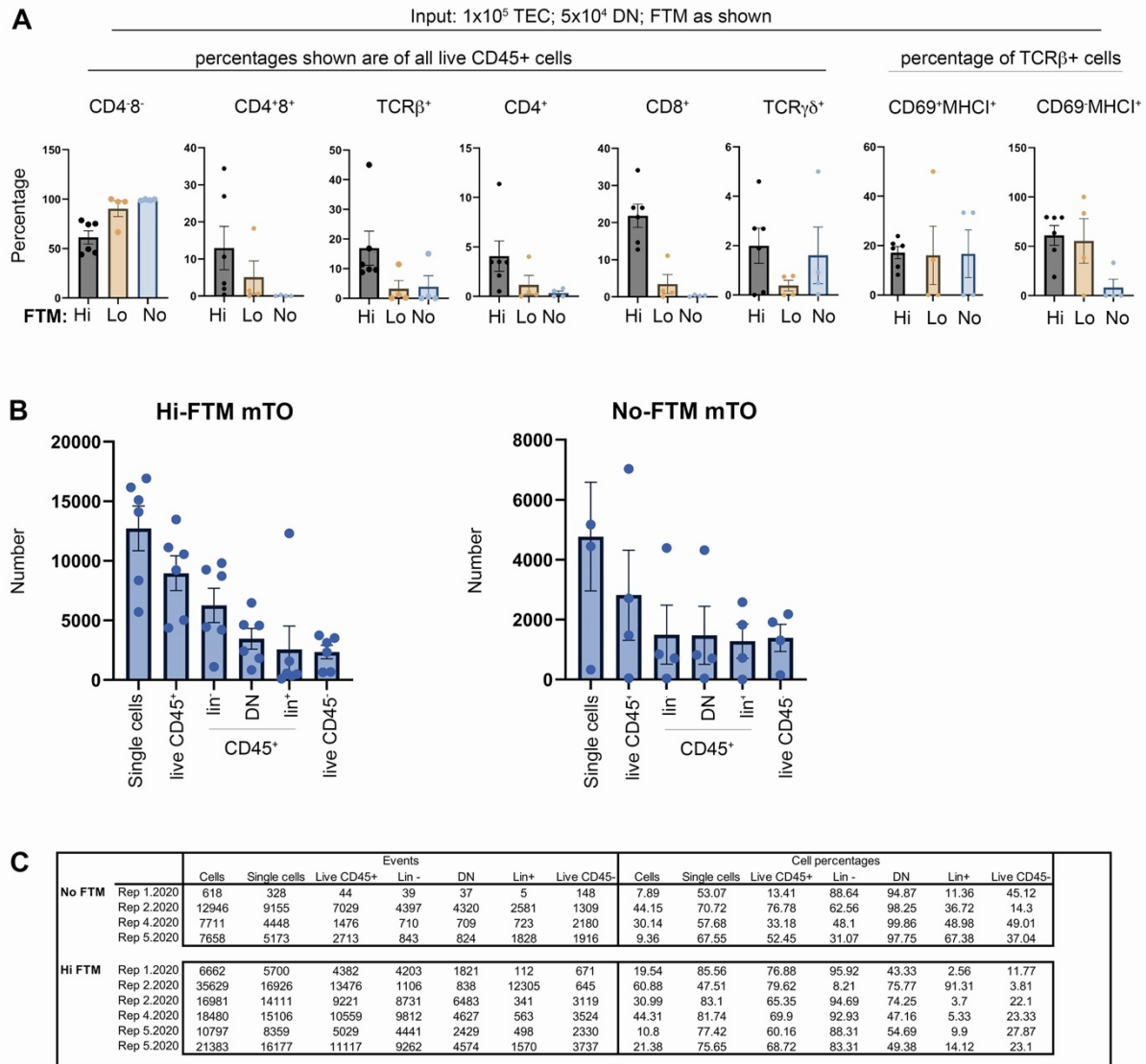
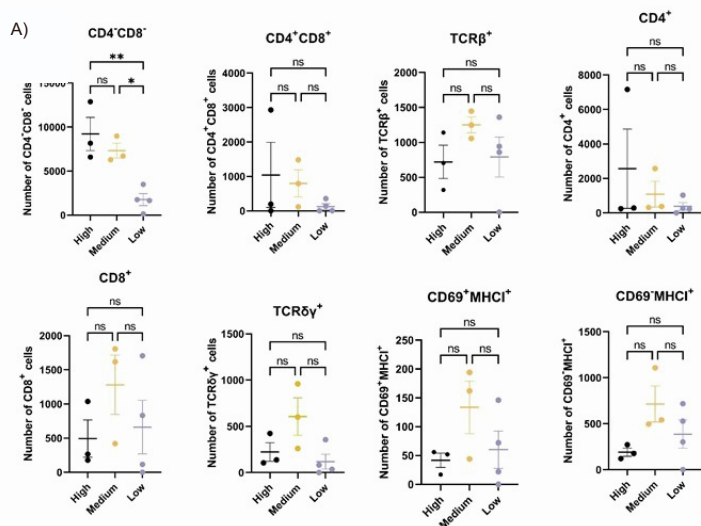


Figure S2. Effect of FTM on mTO outputs. mTO were established from E14.5 thymi using the following input conditions: Hi FTM (1×10^5 TEC, 5×10^4 DN, 4×10^4 FTM), Lo FTM (1×10^5 TEC, 5×10^4 DN, 1.5×10^4 FTM) and No FTM (1×10^5 TEC, 5×10^4 DN, 0 FTM) and were cultured for 14 days before analysis of thymocyte populations shown. (A) Plots show mean \pm SEM of percentage for each subset. Each data point represents the cells harvested from one microwell. Percentages shown are after gating on the populations indicated. N = at least 4 independent biological replicates. DN (CD4⁻CD8⁻), DP (CD4⁺CD8⁺), (CD3 ϵ ⁺TCR β ⁺), SP4 (CD4⁺), SP8 (CD8⁺), CD69⁺MHCII⁺, CD69⁻MHCII⁻, $\gamma\delta$ T cells (CD3 ϵ ⁺TCR $\gamma\delta$ ⁺). (B, C) Plots (B) and Table (C) show number of cells in each of the populations shown. Lin = CD11b, CD11c, Gr-1, Nk1.1, B220, EpCAM and Ter119. In No-FTM mTO data, live CD45⁻ cells are TEC; in Hi-FTM mTO data, live CD45⁻ cells are TEC and FTM.



B)

	Single cells	Live CD45 ⁺ Lin ⁻	TCRβ ⁺	CD69 ⁺ MHCi ⁺	CD69 ⁻ MHCi ⁺	TCRγδ ⁺	SP4 (CD4 ⁺)	DP	SP8 (CD8 ⁺)	DN
High number	73.7 ± 27%	76.4 ± 4.9%	5.3 ± 1%	5.9 ± 1%	32.2 ± 11.8%	1.6 ± 0.5%	17 ± 14.3%	6.1 ± 5.5%	3.4 ± 1.35%	73.6 ± 12%
Medium number	78.1 ± 5.2%	77.5 ± 3.15	12 ± 1.4%	10 ± 3.3%	54.2 ± 9%	5.8 ± 2.1%	11.3 ± 8.1%	7.1 ± 3.1%	12.1 ± 4.1%	70 ± 1.6%
Low number	73.8 ± 14.4%	68.2 ± 13.5%	21.6 ± 7.5%	5.4 ± 2.5%	36 ± 12.9%	2.5 ± 1.3%	12.2 ± 8.4%	2.8 ± 1.6%	15.4 ± 7.8%	69.71 ± 10%

Figure S3. Effect of total cell number on mTO outputs. mTO were established using the same ratio but different absolute numbers of input cells per well (1.5, 1 or 0.5 x the Hi FTM condition numbers) and were cultured for 14 days before analysis of thymocyte development for the subsets shown. A) Graphs show mean ± SEM of absolute cell numbers recovered per well for the input populations. N=3 independent biological replicates, one with two technical replicates for the Low proportion condition. B) Table shows cell mean ± SEM of percentages of parent gates of defined thymocyte subsets present in High, Medium, Low input number mTOs. All data shown cell numbers after gating on live CD45⁺ cells except the CD69⁺MHCi⁺ and CD69⁻MHCi⁺ populations which are gated on TCRβ⁺ cells. Statistical analysis was one-way ANOVA or Kruskal-Wallis rank test based on Shapiro-Wilk normality test. ns not significant; p > 0.05. DN (CD4⁺CD8⁻), DP (CD4⁺CD8⁺), (CD3ε⁺TCRβ⁺), SP4 (CD4⁺), SP8 (CD8⁺), CD69⁺MHCi⁺, CD69⁻MHCi⁺, γδ T cells (CD3ε⁺TCRγδ⁺).

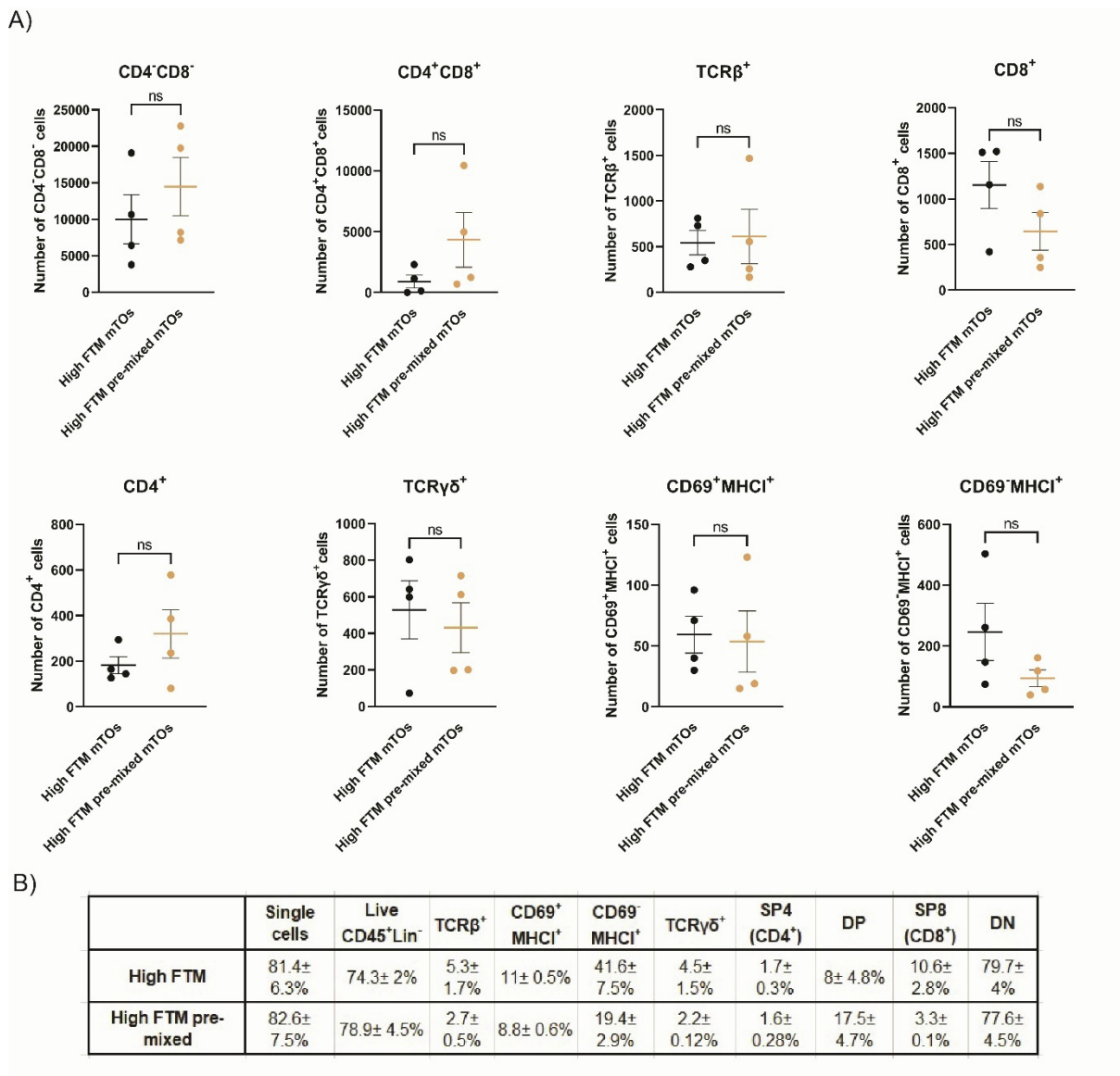


Figure S4. Effect of pre-mixing input cells on mTO outputs. mTO were established from E14.5 thymi using High FTM conditions with or without pre-mixing of input populations (in the without pre-mixing condition the input cell types were added sequentially) as indicated and were cultured for 14 days before analysis of thymocyte development for the subsets shown. (A) Graphs show mean±SEM. High FTM and High FTM pre-mixed had the same cellular composition (1×10^5 TEC, 5×10^4 DN, 4×10^4 FTM). Each data point represents the cells harvested from one microwell. (B) Table shows mean±SEM for percentages of parent gates of the thymocyte subsets shown in High FTM and High FTM pre-mixed mTOs. N=4 independent biological replicates. Statistical analysis was by unpaired t-test or Mann-Whitney rank test based on Shapiro-Wilk normality test. ns, not significant; $p > 0.05$. DN (CD4⁺CD8⁻), DP (CD4⁺CD8⁺), (CD3ε⁺TCRβ⁺), SP4 (CD4⁺), SP8 (CD8⁺), CD69⁺MHCI⁺, CD69⁺MHCI⁺, γδ T cells (CD3ε⁺TCRγδ⁺).

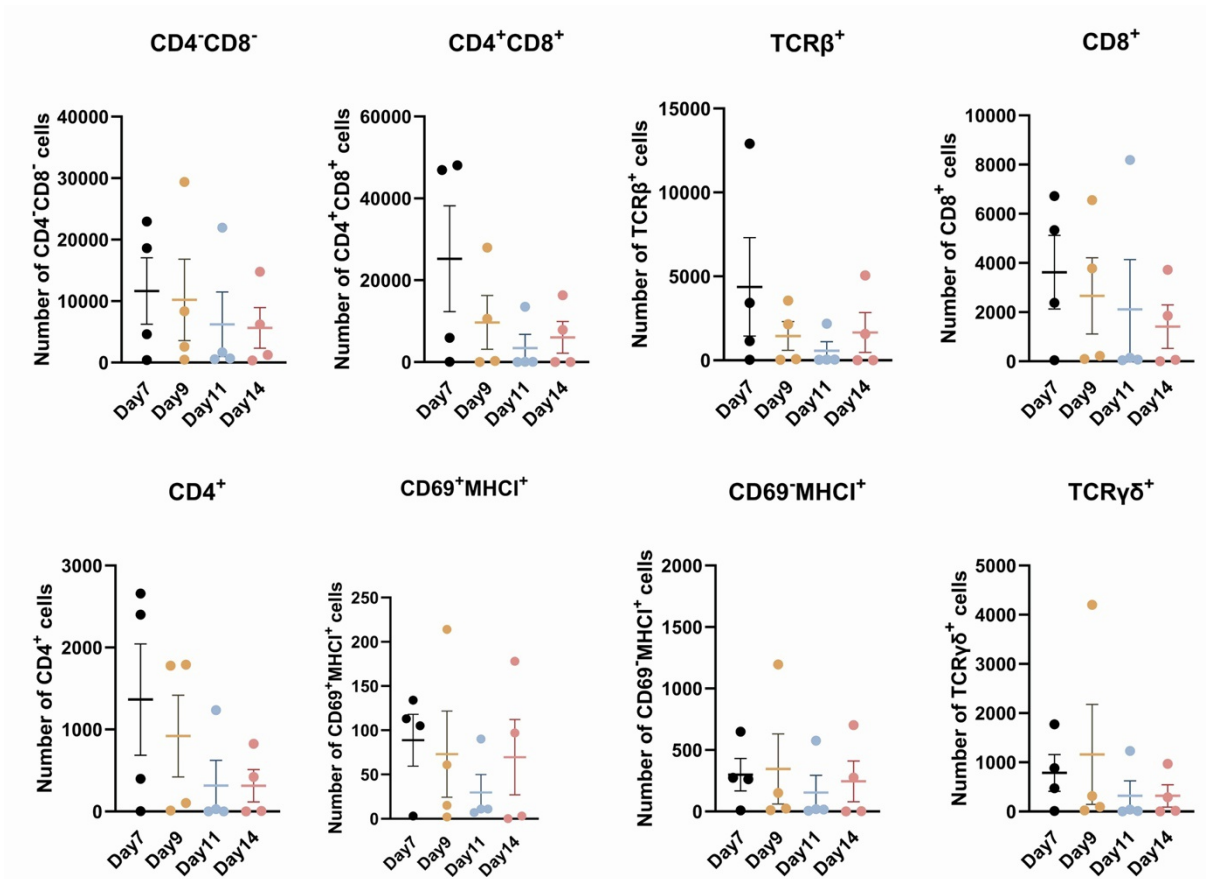
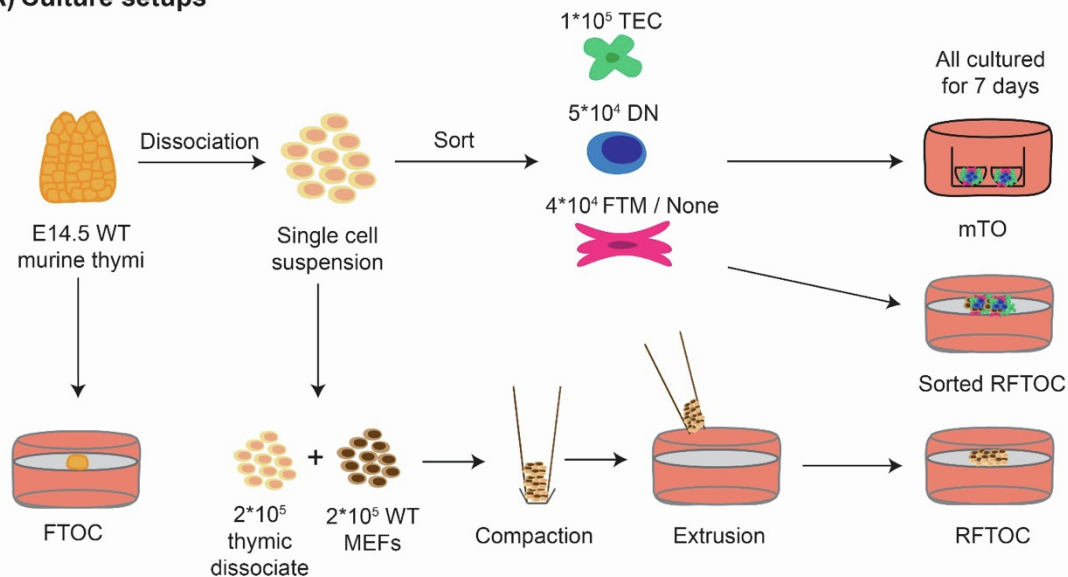
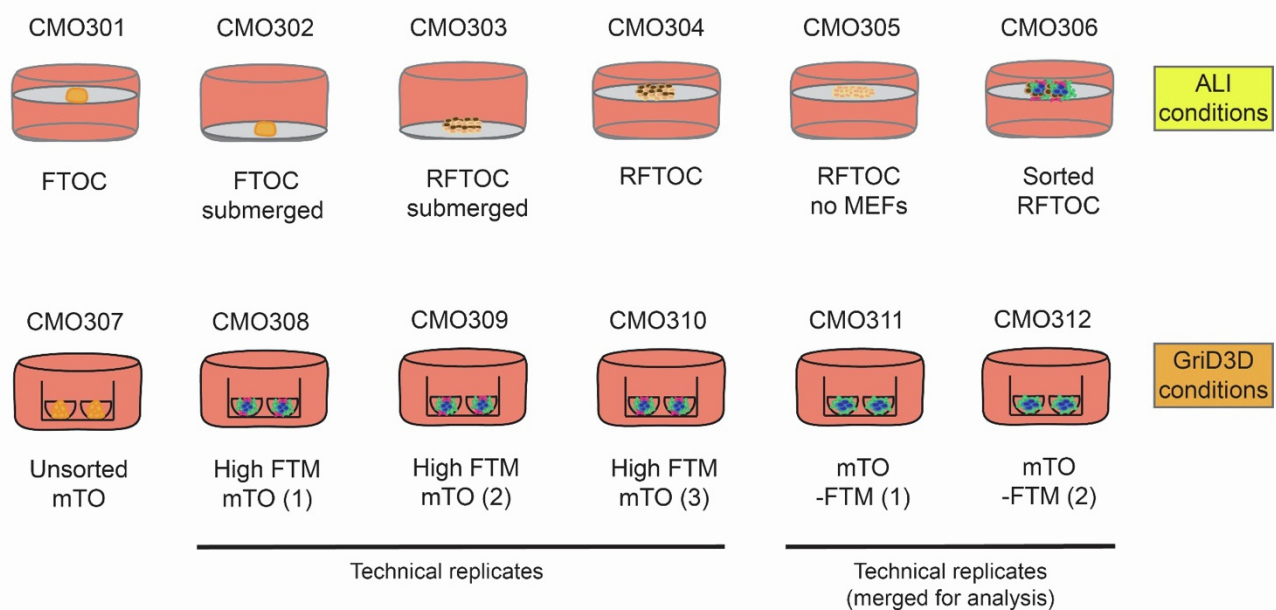


Figure S5. Effect of culture period on mTO outputs. mTO were established from E14.5 thymi using Hi FTM conditions and cultured for the time-periods indicated before analysis of thymocyte development for the subsets shown. (A) Graphs show mean±SEM. Each data point represents the cells harvested from one microwell. N=4 independent biological replicates. DN (CD4⁺CD8⁻), DP (CD4⁺CD8⁺), (CD3ε⁺TCRβ⁺), SP4 (CD4⁺), SP8 (CD8⁺), CD69⁺MHCII⁺, CD69⁺MHCI⁺, γδ T cells (CD3ε⁺TCRγδ⁺).

A) Culture setups



B) CMO assignments



C) Sample preparation

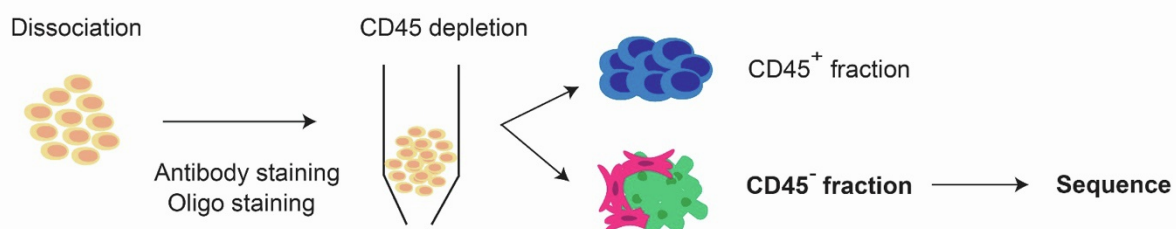


Figure S6. Experimental design for scRNAseq analysis.

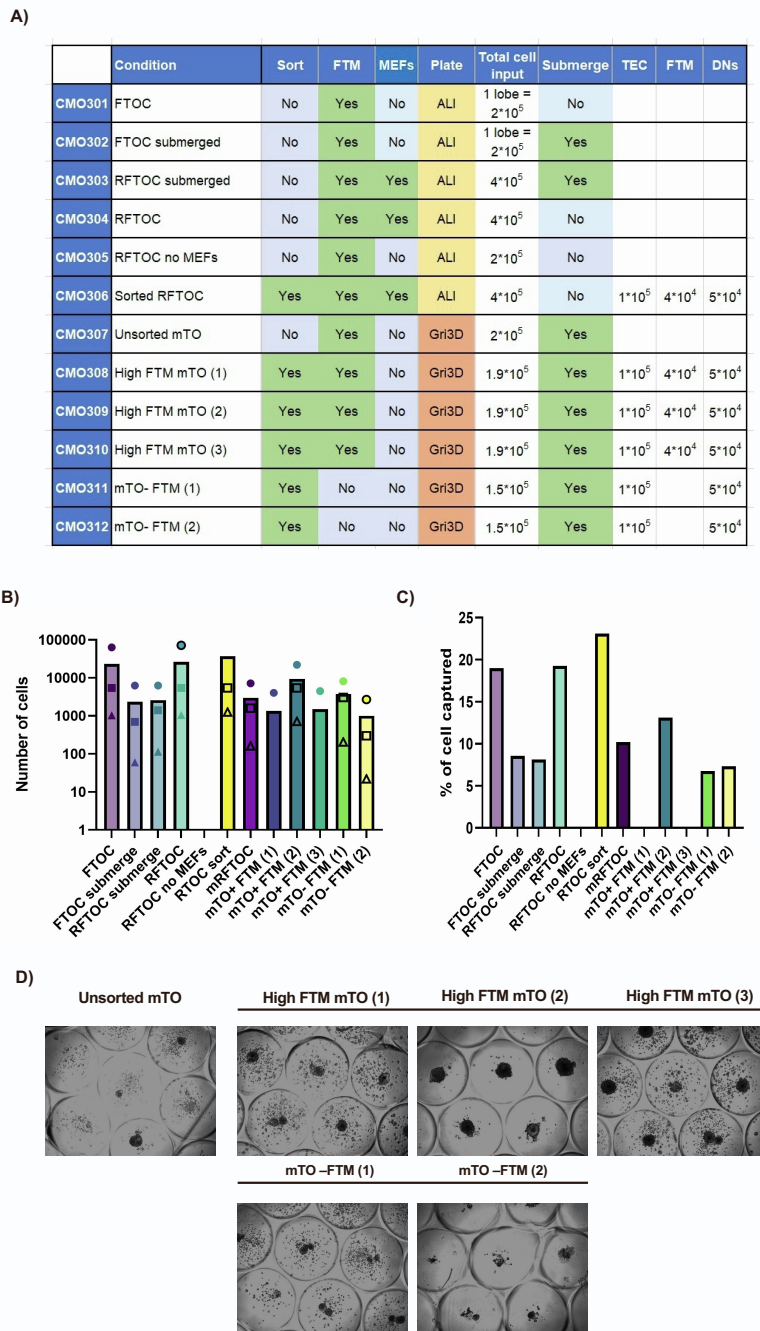


Figure S7. Cell inputs and outputs from ‘Watchbreaker’ scRNAseq experiment. (A) Table showing details of each experimental condition set up for the 10x experiment. (B, C) Graphs show (B) total number of cells counted (circle), loaded on the chip (square) and sequenced (triangle) for each condition and (C) percentage of cells captured by sequencing for each of the experimental conditions; capture efficiency calculated by the ratio of cells sequenced/ cells counted. Note that due to clumping during sample preparation the proportion of cells captured by sequencing is relatively low; this explains the lack of recovery of cells from the mTO (1) and mTO (3) conditions. (D) Images show representative microwells for each of the mTO conditions.

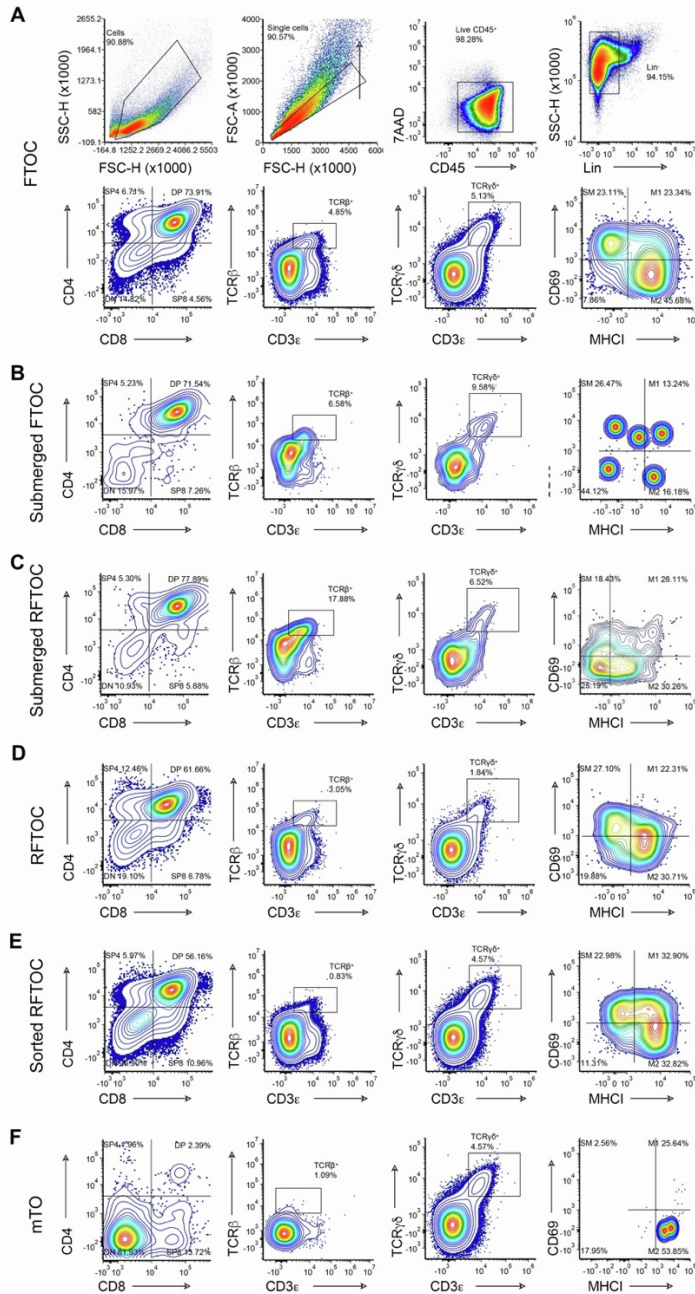


Figure S8. Thymocyte development in different conditions in the ‘Watchbreaker’ 10x experiment. Plots show thymocyte subset analysis of CD45⁺ cells from the conditions shown after seven days of culture. Markers are as shown. (A) Plots show data from FTOC condition (CMO301), including gating strategy. (B-F) Plots show data from the conditions shown; Submerged FTOC (CMO302), Submerged RFTOC (CMO303), RFTOC (CMO304), Sorted RFTOC (CMO306), mTO replicate 2 (CMO309). Note that no DN to DP progression was observed in the following conditions, and therefore those data are not shown: RFTOC without MEFs (CMO305), mTO replicate 1 (CMO308), mTO replicate 3 (CMO310), mTO without FTM replicates 1 and 2 (CMO311 and CMO312). Among these, a DN population was present in all of these conditions except RFTOC without MEFs (CMO305) and the two mTO without FTM replicates. Very few cells were recovered from the unsorted mTO condition (CMO307) those data are also not shown.

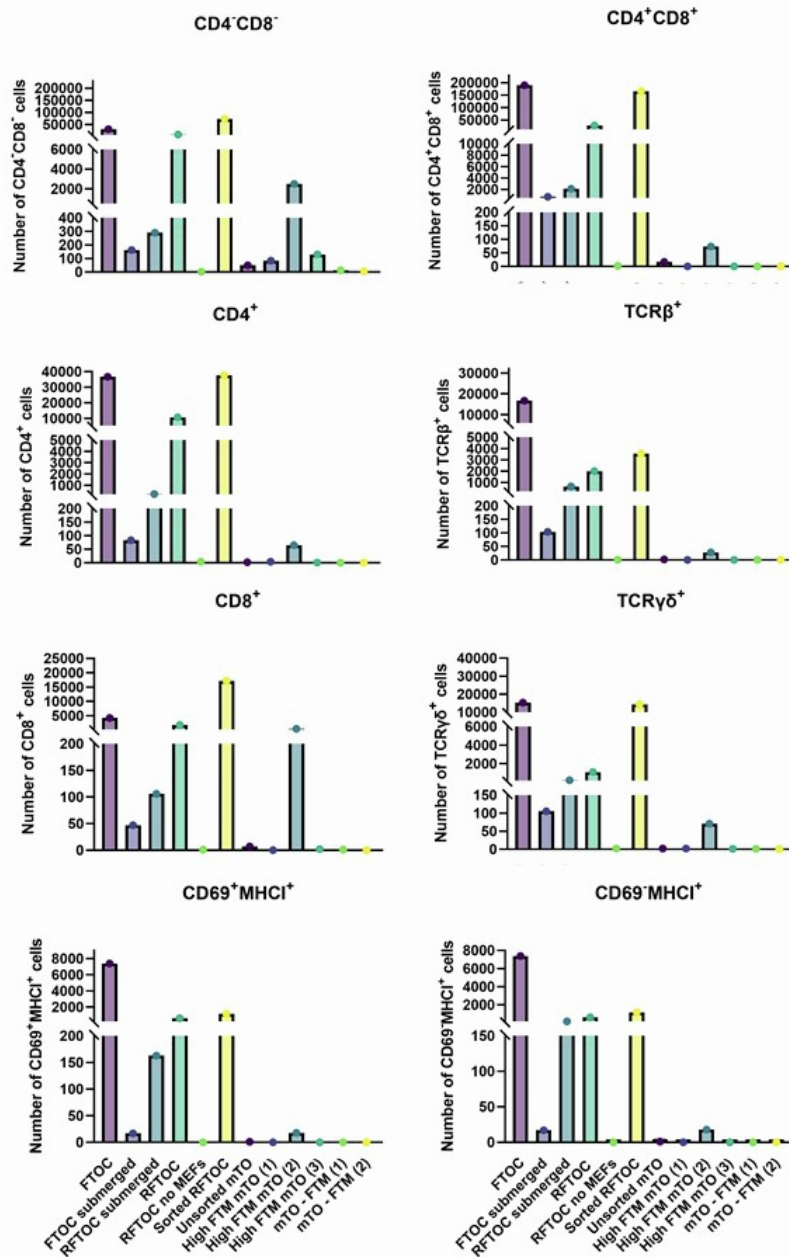


Figure S9. Thymocyte subset numbers in each Watch-breaker condition in the ‘Watchbreaker’ 10x experiment. FTOC, RFTOC and mTO were established as described in Figure S6 and were cultured for 7 days, after which thymocyte development was assessed by analysing the CD45⁺ population for the following subsets (see Figure S8 for flow cytometry plots): DN (CD4⁻CD8⁻), DP (CD4⁺CD8⁺), (CD3ε⁺TCRβ⁺), SP4 (CD4⁺), SP8 (CD8⁺), CD69⁺MHCII⁺, CD69⁺MHCII⁻, γδ T cells (CD3ε⁺TCRγδ⁺). A) Graphs show cell numbers recovered for each subset, for each condition. N=1. B) Graphs show percentages of parent gates present in each condition, for the subsets shown.

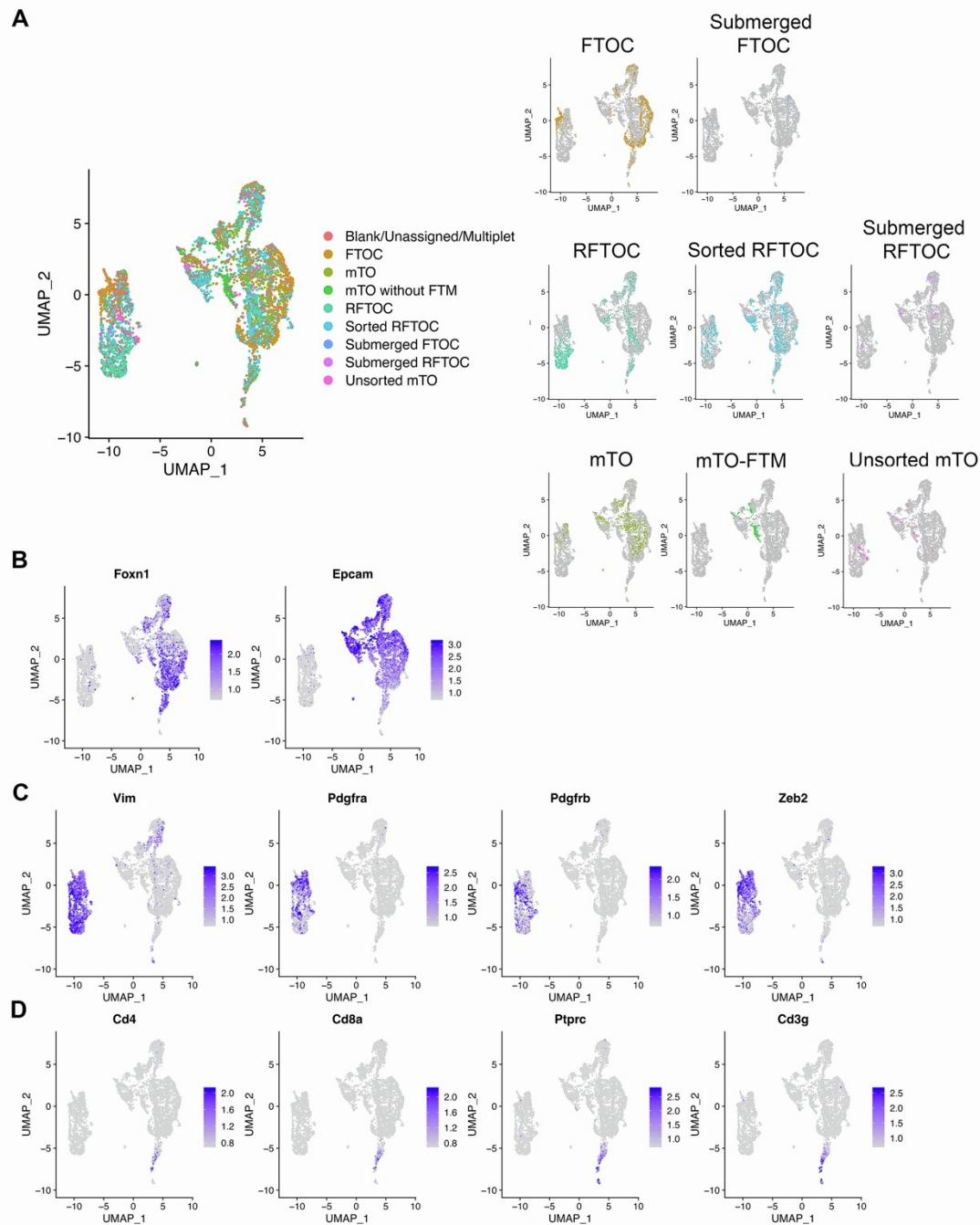


Figure S10. Dimensional reduction showing scRNAseq data from all cells captured from all conditions. (A) UMAP shows distribution of cells from each condition across the combined dataset. Data shown are the 4919 cells remaining after initial quality control. (B-D) Plots show distribution across combined dataset of markers for TEC (B; *Foxn1*, *Epcam*), mesenchymal cells (C; *Pdgrfra*, *Pdgrfb*, *Vim*, *Zeb2*) and thymocytes (D; *Cd3g*, *Cd4*, *Cd8a*, *Prprc*).

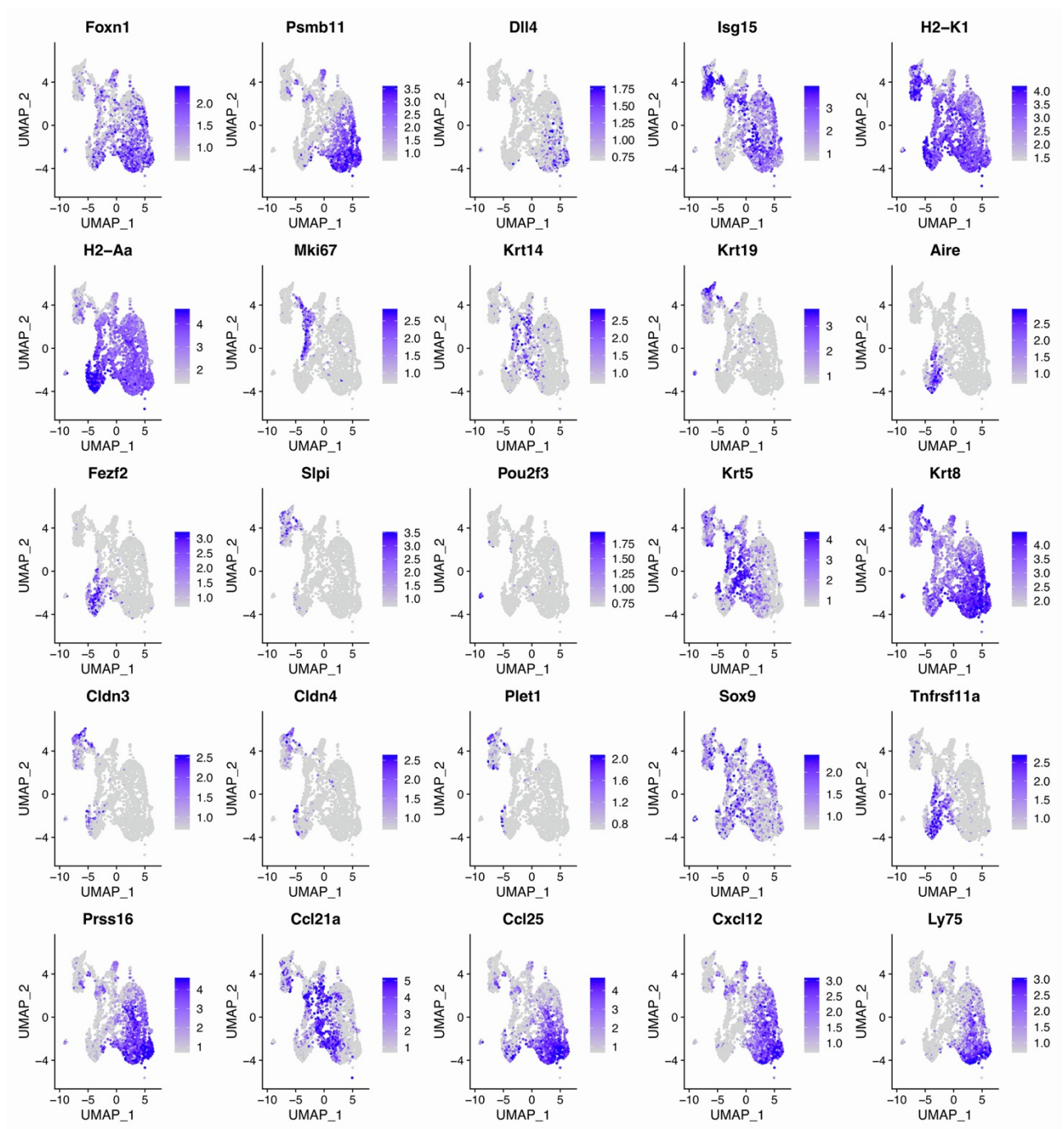


Figure S11. Distribution of markers across TEC. UMAPs show distribution of the markers shown across all TEC in the FTOC, RFTOC, sorted RFTOC, mTO and no-FTM mTO conditions.

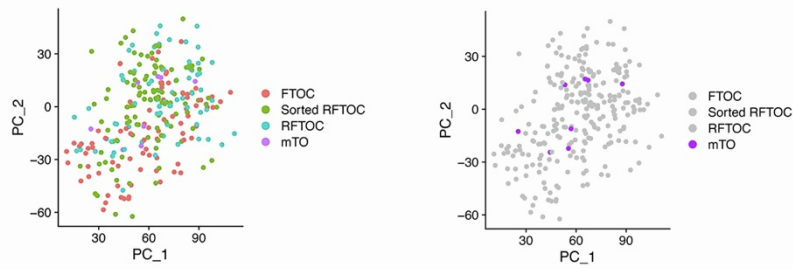
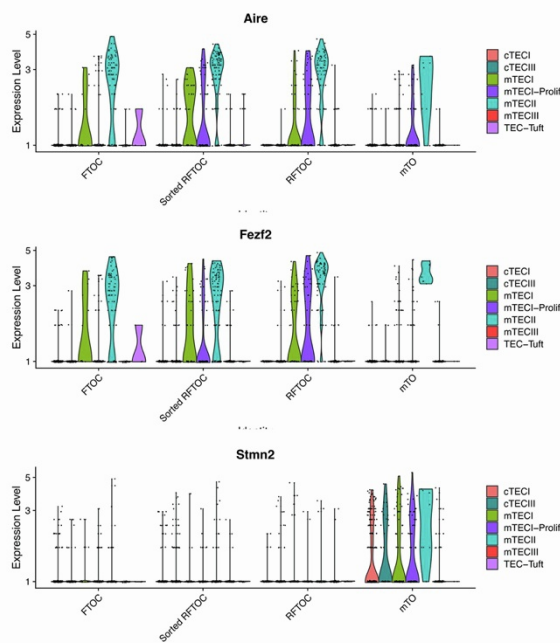
A**B**

Figure S12. Analysis of mTECII subset across four Watchbreaker conditions. (A) PCA shows distribution of mTECII cells in FTOC, RFTOC, Sorted RFTOC and mTO. **(B)** Violin plots showing expression profiles of Aire, Fezf2 and Stmn2 in the different TEC subsets, for each of the above four conditions.

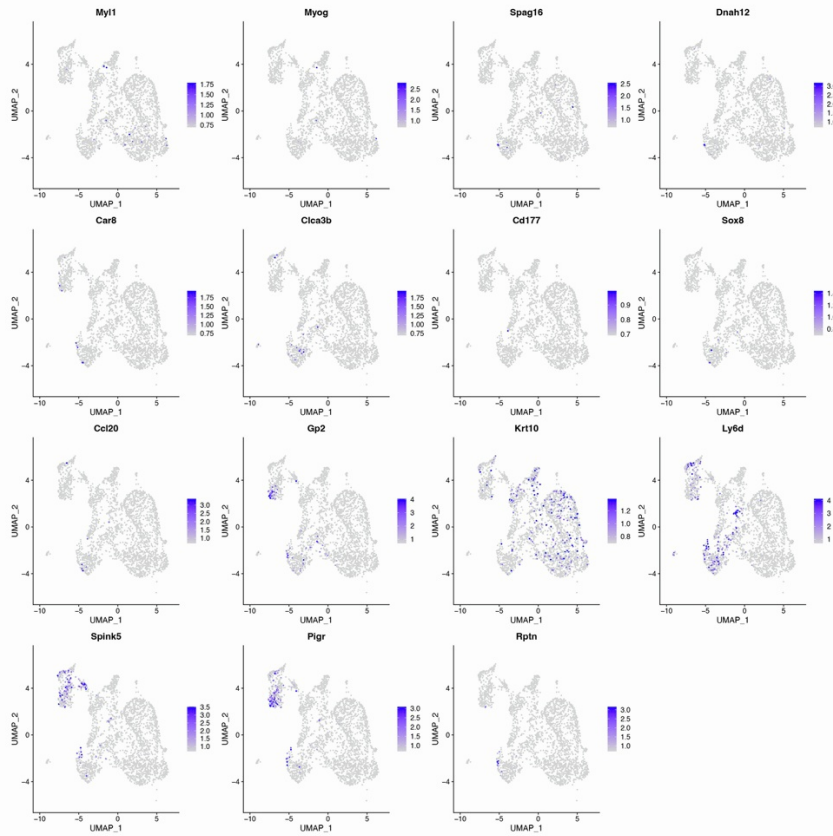
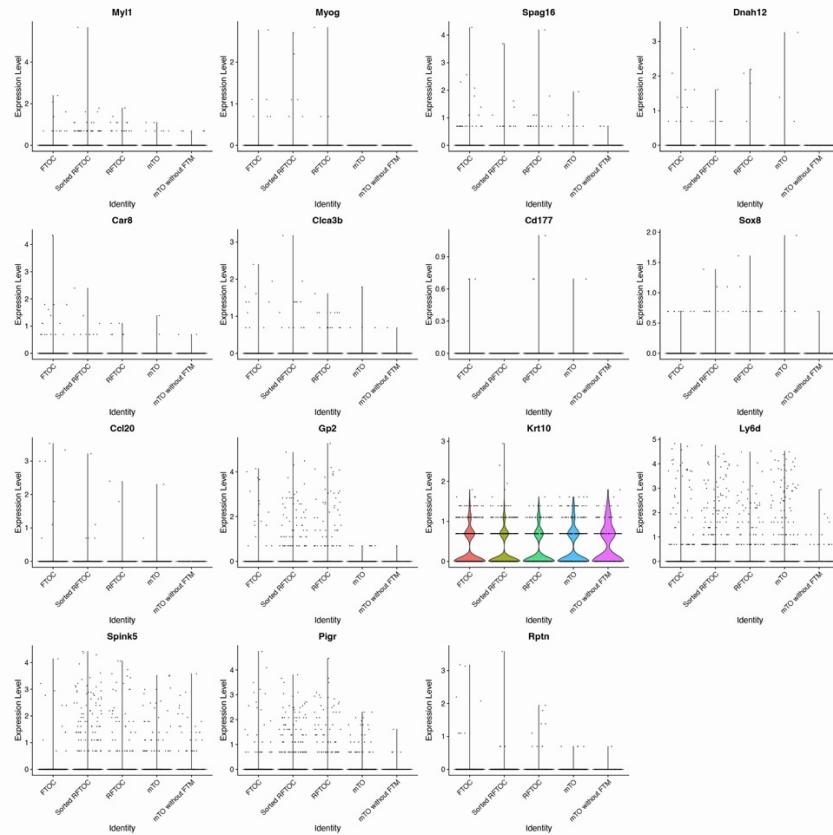
A**B**

Figure S13. Analysis of mimetic TEC markers across five Watchbreaker conditions. (A) UMAPs and **(B)** Violin plots showing expression profiles of the markers shown, across the FTOC, sorted RFTOC, RFTOC, mTO and no-FTM mTO conditions.

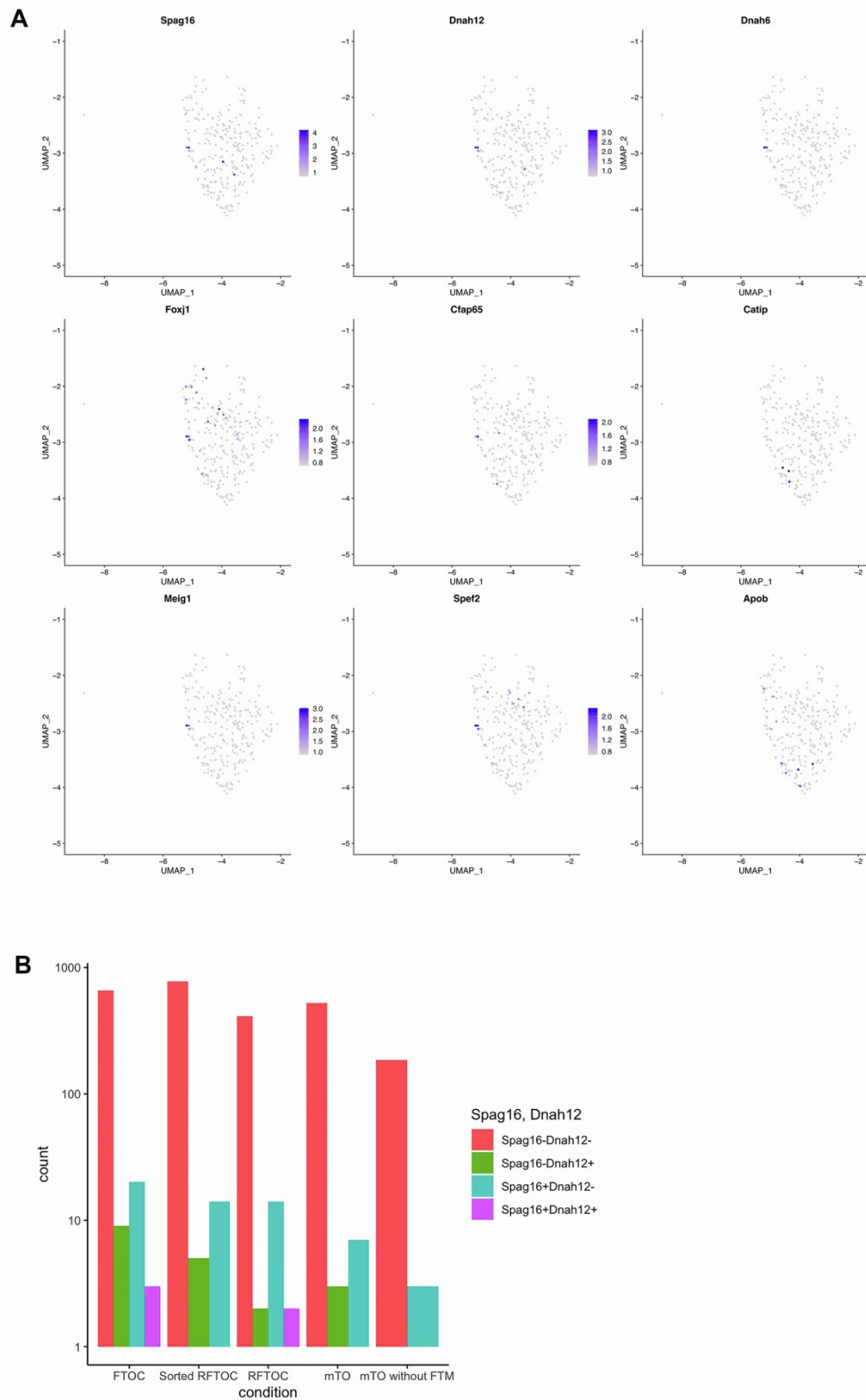


Figure S14. Analysis of CilTEC markers among mTECII, across all Watchbreaker conditions. (A) UMAPs show distribution of CilTEC markers within the mTECII cluster, **(B)** plot shows number of cells with each phenotype in each of five Watchbreaker conditions.

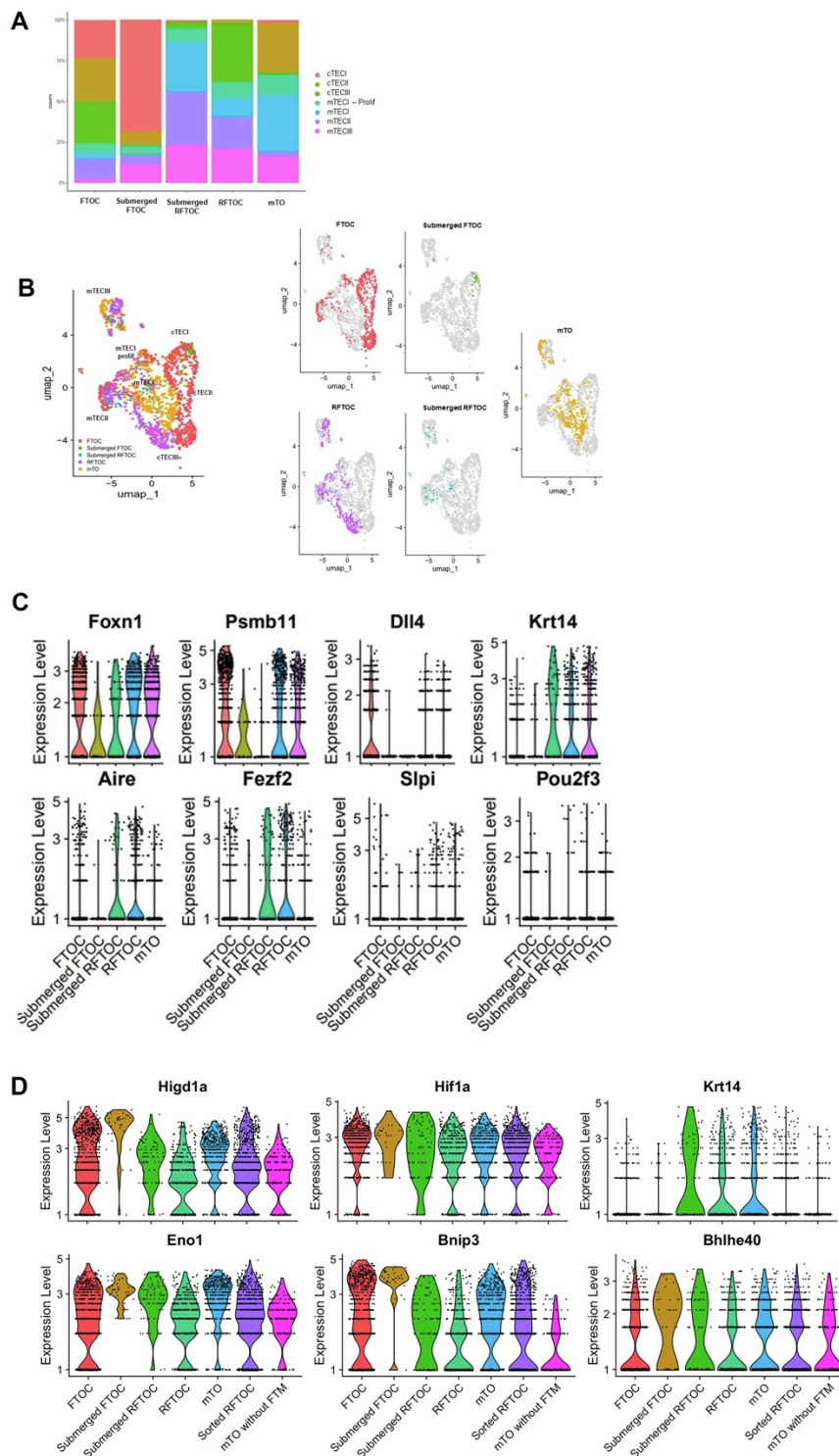


Figure S15. Effect of submersion on cell distribution and gene expression in FTOC and RTOC. **A, B)** Distribution of cell types in the FTOC, Submerged FTOC, Submerged RFTOC, RFTOC, and mTO conditions. UMAPs in (B) show combined data from the conditions shown (left panel) and distributions of TEC in individual conditions (middle and right panels). **C, D)** Violin plots show the expression profiles of the genes shown in the FTOC, Submerged FTOC, Submerged RFTOC, RFTOC, and mTO conditions. Plots in (C) show TEC markers; plots in (D) show hypoxia response genes.

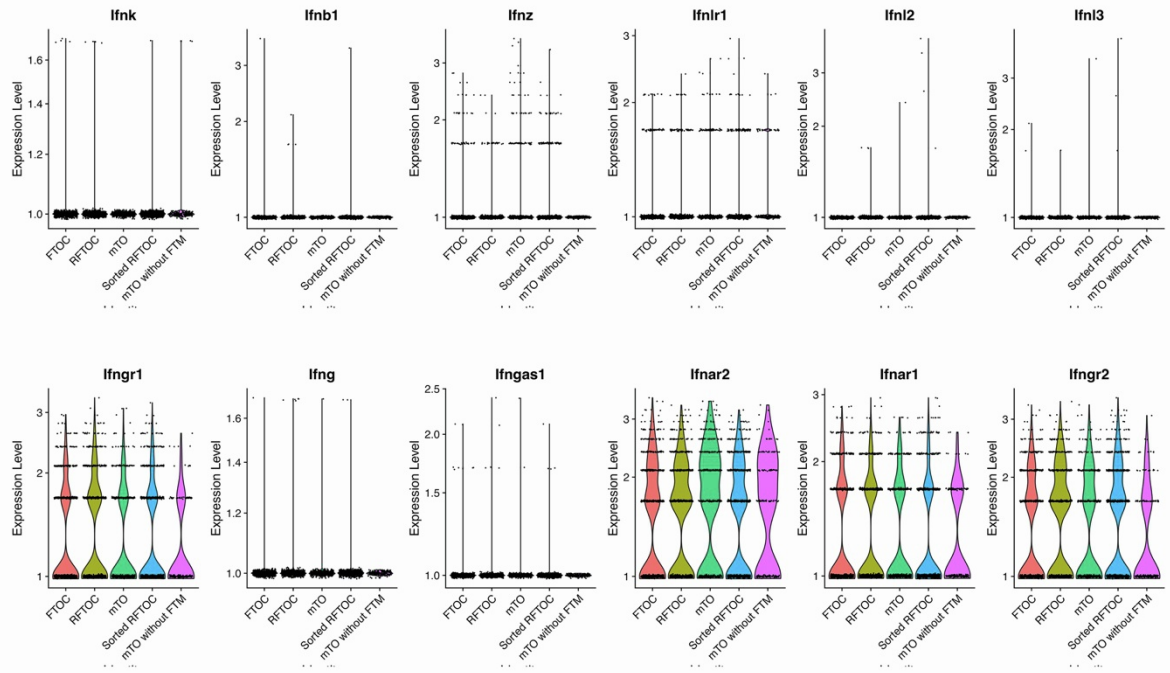
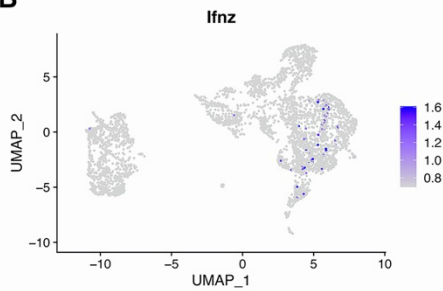
A**B**

Figure S16. Expression of IFN family and IFN receptor genes in selected ‘Watch-breaker’ conditions. (A) Violin plots show the expression profiles of the genes shown in the FTOC, Sorted RFTOC, RFTOC, mTO and mTO-FTM conditions. Analyses show gene expression across all cells in the dataset, including mesenchymal cells. IFN α and IFN γ receptors were expressed, but expression of the IFN family genes analysed was not detected, or was detected in only very few cells in each condition (*Ifnz*). *Ifna* was not detected. **(B)** UMAP shows distribution of *Ifnz*+ cells.

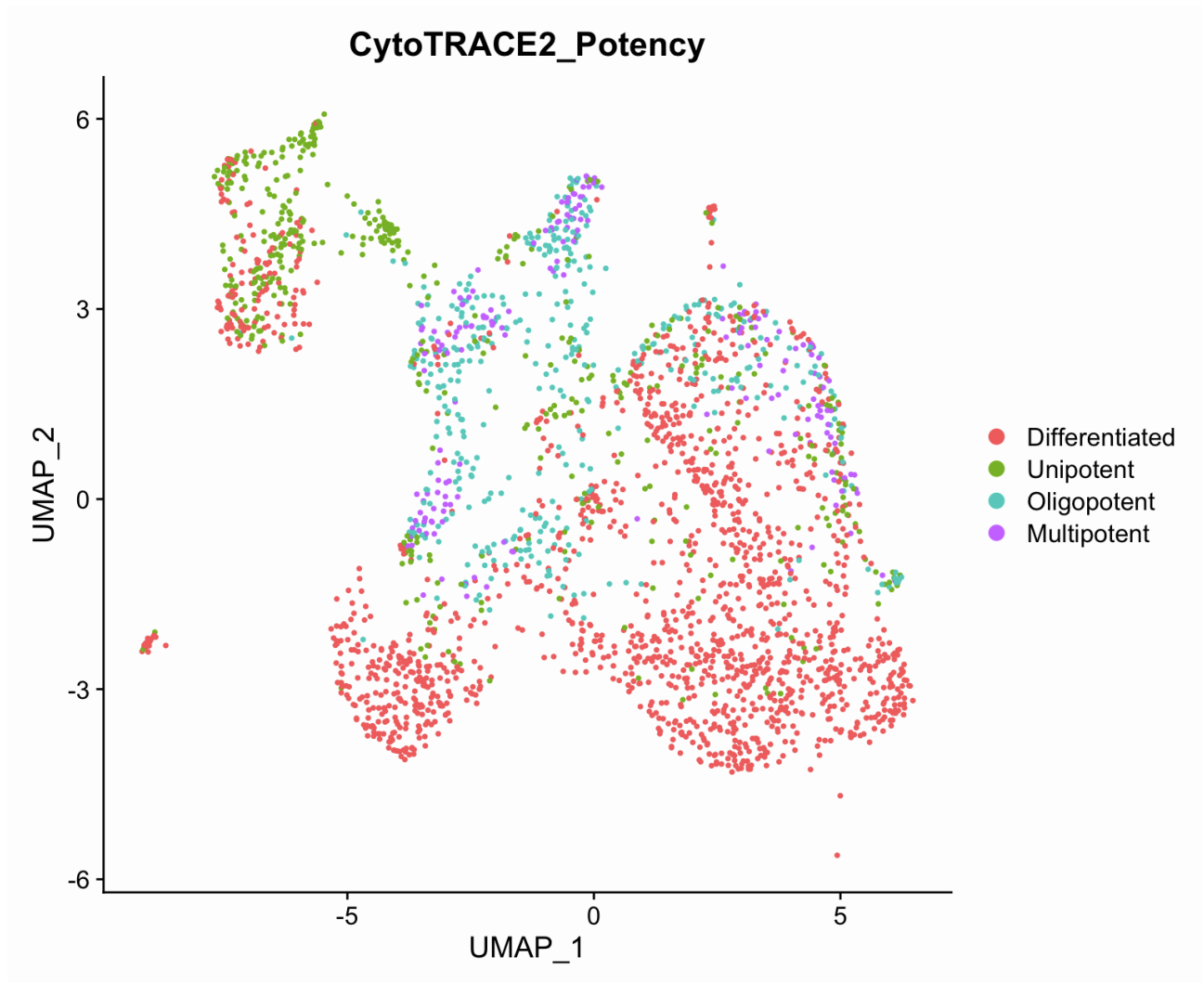


Figure S17. CytoTRACE2 analysis across all 'Watch-breaker' conditions. The UMAP projection is as in Figure 6. Colours indicate cell potency as predicted by the CytoTRACE2 algorithm. The mTECIII cluster is predicted to contain both unipotent progenitors and differentiated cells.

Supplemental Tables

<i>Transgene</i>	<i>Orientation</i>	<i>Sequence</i>
Cxcl12 WT	Forward	5' CTG GTT TTC GCC TCT AAA GC
Cxcl12 Tg	Forward	5' TCG GCA AAA TCC CTT ATA AAT C
Cxcl12	Reverse	5' CAG AGC TGC GAG CCT TTC
Rank Venus WT	Forward	5' CTGCGTGCTGCTCGTTCCAC
Rank Venus Tg	Forward	5' GAAGAACGGCATCAAGGCCAACTTC
Rank Venus	Reverse	5' CTGTACATACAATCTTACTGAGGGTCGC
GFP	Forward	5' TAT ATC ATG GCC GAC AAG CA
GFP	Reverse	5' GAA CTC CAG CAG GAC CAT GT

Table S1. Primers used to genotype transgenic lines.

	Antigen	Fluorophore	Dilution	Supplier	Cat. Number	Clone
Flow cytometric isolation of TEC, DN thymocytes, FTM and EC from E14.5 thymic lobes	EpCAM	FITC	1:1000	BioLegend	118208	G8.8
	PDGFR α	APC	1:2000	BioLegend	35908	APA5
	PDGFR β	APC	1:2000	BioLegend	136007	APB5
	TER119	PE	1:3000	BioLegend	116208	TER-119
	CD31	Pe/Cy7	1:1600	BioLegend	102523	MEC13.3
	CD45	APC-eFLuor780	1:1000	eBioscience	47-0451-82	30-F11
	DAPI	-	0.5 μ g/ml	Life Technologies	D1306	-
Flow cytometric isolation of LMPPs from E14.5 fetal liver	DAPI	-	0.5 μ g/ml	Life Technologies	D1306	-
	CD5	FITC	1:1000	BioLegend	100605	53-7.3
	CD19	FITC	1:500	BioLegend	152403	1D2
	Gr1	FITC	1:800	BioLegend	108405	RB6-8C5
	NK1.1	FITC	1:800	BD Biosciences	553164	PK136
	CD45R/B220	FITC	1:800	BioLegend	103206	RA3-6B2
	TER-119	FITC	1:800	eBioscience	11-5921-85	TER-119
	F4/80	FITC	1:1600	BioLegend	2BM8	123108
	CD135 (Flt3)	APC	1:50	BioLegend	135310	A2F10
	Sca-1	PE	1:2000	BioLegend	108107	D7
	CD117 (cKit)	PE/Cy7	1:1600	BioLegened	105813	2B8
Flow cytometric analysis of T cell subsets from mTOs	7AAD	-	1:200	BioLegend	420403	-
	CD11b	FITC	1:800	BioLegend	101205	M1/70
	CD11c	FITC	1:800	BioLegend	117305	N418
	Gr1	FITC	1:800	BioLegend	108405	RB6-8C5
	NK1.1	FITC	1:800	BD Biosciences	553164	PK136
	CD45R/B220	FITC	1:800	BioLegend	103206	RA3-6B2

	TER-119	FITC	1:800	eBioscience	11-5921-85	TER-119
	EpCAM	FITC	1:800	BioLegend	118208	G8.8
	CD4	PE	1:800	BioLegend	100512	RM4-5
	CD8α	APC	1:400	eBioscience	17-0081-82	53-6.7
	CD3ε	BV785	1:100	BioLegened	100355	145-2C11
	TCRβ chain	PE/Cy7	1:100	BioLegend	109222	H57-597
	CD45	APC/eFluor 780	1:800	eBioscience	47-0451-82	30-F11
	γ/δTCR	BV605	1:400	BioLegend	118124	GL3
	MHC1 (H-2k)	BV510	1:400	BioLegend	116523	AF6-88.5
	CD69	BV421	1:100	BioLegend	104528	H1.2F3
IHC of in vitro cultures	Vimentin	-	1:250	Abcam	ab92547	Abcam (rabbit)
	MHCII	-	1:200	Abcam	ab15630	ER-TR3
	β5t	-	1:100	MBL	PD021	Polyclonal
	DLL4	-	1:50	BioLegend	130802	HMD4-1
	MHCI	-	1:200	BDBioscience	550550	AF6-88.5
	HOECHST	-	1:1000	Life Technologies	62249	
	Anti-Rabbit secondary	Alexa Fluor 568	1:1000	Invitrogen	A-11011	
	Anti-Rat secondary	Alexa Fluor 647	1:1000	Invitrogen	A-21247	

Table S2. Antibodies used in panels for flow cytometry and immunohistochemistry. Table shows the name, associated fluorophore where appropriate, supplier and clone number. DAPI, (4',6-Diamidino-2-Phenylindole, Dihydrochloride); IHC, immunohistochemistry.

Antibody	Barcoded Reagent	Dilution	Supplier	Cat. Number
UEA1-Biotin	TotalSeq™-SAV-Pe-B0952	1:1500	Vector Laboratories	B-1065
MHCII (α-mouse I-A/I-E)	TotalSeq™ - B0117	1:10000	BioLegend	107657
CD40	TotalSeq™ - B0903	1:3200	BioLegend	124639
CD80	TotalSeq™ - B0849	1:3200	BioLegend	104757
EpCAM	TotalSeq™ - B0449	1:800	BioLegend	118247
CD45	Beads	1:10	Miltenyi Biotec Inc.	130-052-301

Table S3. Cell staining reagents used in 10x sequencing experiment.

TEC subset	Markers	Reference
cTECneg, cTECI and cTECIII	<i>Psmb11, Cxcl12, Prss16</i>	Kernfeld et al 2018 ¹ , Baran-Gale et al. 2020 ²
mTECI	<i>Krt5, Ccl21a</i>	Kernfeld et al 2018 ¹ , Baran-Gale et al. 2020 ²
mTECI prolifer	<i>Mki67, Ccna2, Pbk</i>	Yayon et al. 2024 ³ , Baran-Gale et al. 2020 ²
mTECII	<i>Aire, H2-Aa</i>	Bornstein et al. 2018 ⁴
mTECIII	<i>Pigr, Ly6d</i>	Bornstein et al. 2018 ⁴ , Givony et al 2023 ⁵
TEC-Tuft	<i>Avil, Spink5</i>	Baran-Gale et al. 2020 ²
CiITEC	<i>Spag16, Dnah12</i>	Givony et al 2023 ⁵

Table S4: List of genes used to identify TEC subpopulations annotated in Figures 5, 6 and S10-17.

References

1. Kernfeld, E.M., Genga, R.M.J., Neherin, K., Magaletta, M.E., Xu, P., and Maehr, R. (2018). A Single-Cell Transcriptomic Atlas of Thymus Organogenesis Resolves Cell Types and Developmental Maturation. *Immunity* 48, 1258-1270 e1256. 10.1016/j.immuni.2018.04.015.
2. Baran-Gale, J., Morgan, M.D., Maio, S., Dhalla, F., Calvo-Asensio, I., Deadman, M.E., Handel, A.E., Maynard, A., Chen, S., Green, F., et al. (2020). Ageing compromises mouse thymus function and remodels epithelial cell differentiation. *Elife* 9. 10.7554/eLife.56221.
3. Yayon, N., Kedlian, V.R., Boehme, L., Suo, C., Wachter, B.T., Beuschel, R.T., Amsalem, O., Polanski, K., Koplev, S., Tuck, E., et al. (2024). A spatial human thymus cell atlas mapped to a continuous tissue axis. *Nature* 635, 708-718. 10.1038/s41586-024-07944-6.
4. Bornstein, C., Nevo, S., Giladi, A., Kadouri, N., Pouzolles, M., Gerbe, F., David, E., Machado, A., Chuprin, A., Toth, B., et al. (2018). Single-cell mapping of the thymic stroma identifies IL-25-producing tuft epithelial cells. *Nature* 559, 622-626. 10.1038/s41586-018-0346-1.
5. Givony, T., Leshkowitz, D., Del Castillo, D., Nevo, S., Kadouri, N., Dassa, B., Gruper, Y., Khalaila, R., Ben-Nun, O., Gome, T., et al. (2023). Thymic mimetic cells function beyond self-tolerance. *Nature* 622, 164-172. 10.1038/s41586-023-06512-8.